

Predicting and optimizing the territory of blood–brain barrier opening by superselective intra-arterial cerebral infusion under dynamic susceptibility contrast MRI guidance

Mirosław Janowski^{1,2,3,4,*}, Piotr Walczak^{1,2,5,*} and Monica S Pearl^{6,7}

Abstract

Interventional neuroradiology techniques are minimally invasive and allow for superselective drug delivery to specific brain regions. The passage of most agents, however, is impaired by the blood–brain barrier (BBB). Despite its discovery over 40 years ago, hyperosmotic BBB opening (BBBO) remains highly variable, preventing its widespread implementation. Here, we report on a technique that enables the prediction and optimization of the BBBO territory. We found that the microcatheter tip position and the speed of hyperosmolar mannitol injection, both major determinants of the targeted territory, can be modulated in real-time as guided by trans-catheter perfusion MRI.

Keywords

Blood–brain barrier opening, intra-arterial, mannitol, MRI

Received 24 January 2015; Revised 7 July 2015; Accepted 23 September 2015

Introduction

The blood–brain barrier (BBB) is a dynamic system that regulates transport of materials between the blood, brain, and cerebrospinal fluid. An intact BBB effectually prevents passage of ionized water-soluble compounds with molecular weights exceeding 180 Da¹ and is a major obstacle for drug delivery to the central nervous system (CNS), partly because most agents have molecular weights between 200 and 1200 daltons.² Interventional neuroradiology techniques are minimally invasive and allow for superselective delivery of therapeutic agents to specific CNS targets.³ In the presence of an intact BBB, safe, effective, and most importantly predictable opening of the BBB is a critical element to increase therapeutic efficacy for multiple CNS pathologies, including tumors and neurodegenerative disorders.⁴ Osmotic BBB opening (BBBO) is a proven method that results in increased BBB permeability; however, this technique remains controversial due to its variability and the lack of non-invasive methods for real-time intra-procedural validation.

Fluoroscopic x-ray-based digital subtraction angiography (DSA) is the gold standard technique for

catheter-based neurointerventions. Methods for assessing BBBO are currently not available with this modality; however, contrast-enhanced MRI is excellent for

¹Division of MR Research, Russell H. Morgan Department of Radiology and Radiological Science, The Johns Hopkins University School of Medicine, Baltimore, MD, USA

²Cellular Imaging Section and Vascular Biology Program, Institute for Cell Engineering, Johns Hopkins University, Baltimore, MD, USA

³NeuroRepair Department, Mossakowski Medical Research Centre, Polish Academy of Sciences, Warsaw, Poland

⁴Department of Neurosurgery, Mossakowski Medical Research Centre, Polish Academy of Sciences, Warsaw, Poland

⁵Department of Radiology, Faculty of Medical Sciences, University of Warmia and Mazury, Olsztyn, Poland

⁶Division of Interventional Neuroradiology, The Johns Hopkins University School of Medicine, Baltimore, MD, USA

⁷Interventional Neuroradiology, Children's National Medical Center, Washington, DC, USA

*The first two authors contributed equally to this work

Corresponding author:

Monica S Pearl, Division of Interventional Neuroradiology, The Johns Hopkins University School of Medicine, 1800 Orleans Street, Bloomberg Building, 7218 Baltimore, MD 21287, USA.
 Email: mmit135@jhmi.edu

that purpose and lacks the exposure to ionizing radiation inherent with DSA. Our objectives were to develop a reproducible, predictable method of BBBO based on intra-arterial (IA) delivery while utilizing the optimal features offered by both modalities. We tested this method in New Zealand white rabbits, which are sufficiently large to enable a transfemoral approach and selective microcatheter access, and used a combination of fluoroscopic and advanced MRI techniques such as dynamic susceptibility contrast (DSC) MRI⁵ to guide intervention. Although the proposed method is tailored to our goal of treating incurable, surgically inoperable tumors such as diffuse intrinsic pontine gliomas (NCT01688401), its applications may extend beyond, as it is a method of predictable, selective delivery for any therapeutic agent to the CNS.

Materials and methods

Anesthesia and animal preparation

The Johns Hopkins University Institutional Animal Care and Use Committee approved this protocol which was performed in compliance with the ARRIVE guidelines. Eight 4-kg New Zealand white rabbits were sedated with intramuscular acepromazine (1 mg/kg) and ketamine hydrochloride (20 mg/kg), after which intravenous access was established through a marginal ear vein. Intravenous propofol (6.44 mg/kg) was then administered to facilitate endotracheal intubation and the rabbits were maintained on 2% isoflurane gas. A 4-French sheath was surgically placed in the right femoral artery. Oxygen saturations and respiratory rates were monitored.

Digital subtraction angiography

Via a transfemoral approach, a 4-French Glide catheter (Terumo, Somerset, NJ) was advanced over a 0.035-in wire and the left vertebral artery was selectively catheterized. Under roadmap guidance, a 1.7-French Prowler 10 microcatheter (Codman Neuro, Raynham, MA) was advanced over a 0.014-inch microwire into the V4 segment (four rabbits) or basilar artery (four rabbits). Microcatheter angiography was performed to confirm position and assess antegrade flow. The catheters were secured in place and maintained on heparinized saline flush (4000 IU heparin/1 l normal saline).

Interventional MRI technique

The rabbits were transported to a 3 T MRI (Magnetom Trio, Siemens) and underwent baseline T2 (TR/TE 1500/105) and T1 (TR/TE 300/9.1) weighted images of the brain. The horizontal plane best displayed the brainstem in its entirety and was chosen as the working view for DSC

enhanced trans-catheter perfusion. IA Feraheme (dissolved in saline at 1:100; 0.3 mg Fe/ml) was infused between 0.001 and 0.1 ml/s for 30 s to assess trans-catheter parenchymal perfusion territory at specific speeds. We started with the lowest speed, and then we were increasing it until the satisfactory parenchymal perfusion was achieved. For controlled contrast agent and drug administration, a standard infusion pump (Harvard apparatus) was utilized.

Real-time GE-echo planar imaging (GE-EPI) images (TE = 36 ms, TR = 3000 ms, FOV = 1080, matrix = 128, and temporal resolution = 3 s.) were obtained for DSC. Immediately after the Feraheme injection, 25% warmed IA mannitol was administered at the optimal rate previously determined by the Feraheme injection. Five minutes after IA mannitol, 1.5 ml of gadolinium (Magnevist, 0.125 mmol/kg) and Evans Blue (EB) 2% (2 mg/kg) were injected intravenously. T1-weighted images were acquired post gadolinium.

To demonstrate the role of microcatheter tip placement, the microcatheter was withdrawn more proximally within basilar artery inside the MR scanner, after which the Feraheme and mannitol infusions were repeated.

Osirix (Pixmeo) and Amira (FEI) software were used for image processing and visualization.

Prediction of BBBO area by assessment of perfusion territory

DSC Feraheme MR images delineated the region of trans-catheter perfusion territory and T1-weighted gadolinium enhanced MR images depicted the region of BBBO. Slice selection was based on the greatest territory of BBBO. Identical slice geometry for T1 and DSC scans facilitated spatial co-registration of the regions of interest and calculation of the surface areas (cm²) of the perfusion territory, BBBO, mismatch areas, and the total brain area of the analyzed slice.

Accuracy of BBBO procedure

For evaluation of the iron oxide infusion as a predictor of the BBBO territory, we segmented and measured the area (cm²) for four brain regions (Figure 1): 1) the overlapping area for both T1 enhancement and DSC MRI hypointensity = true positive (TP); 2) the hypointense area which did not overlap with T1 enhancement = false positive (FP); 3) the area of T1 enhancement which was not hypointense on DSC MRI = false negative (FN); 4) the area of the brain with no signal changes on T1 or T2 = true negative (TN).

Post mortem analysis

The rabbits were perfused with 4% paraformaldehyde solution. The brains were harvested and coronal 1-mm

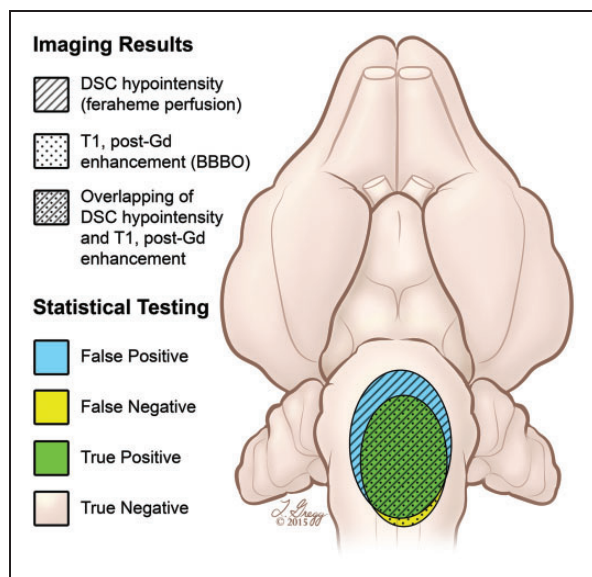


Figure 1. Artistic rendering showing evaluation of the iron oxide infusion as a predictor of the BBBO territory. Horizontal view of the rabbit brain shows the four brain regions that were segmented and measured for assessment of BBBO accuracy. The patterned regions depict the MRI imaging findings from DSC and T1 post-gadolinium weighted sequences. The colored areas show statistical results.

slices were obtained using a brain matrix. The BBBO territory was assessed by EB extravasation.

Statistics

The mean values from seven rabbits for each of the four territories were extracted and were used for further calculations. One rabbit was excluded from calculations due to significant motion artifact, which degraded image quality. We performed standard validity analysis and calculated the positive predictive value (PPV) = $TP/(TP + FP)$, negative predictive value (NPV) = $TN/(TN + FN)$, sensitivity = $TP/(TP + FN)$ and specificity = $TN/(FP + TN)$ for prediction of the BBBO area (T1-weighted) using iron oxide infusion (T2-weighted). The r Pearson correlation coefficient of the territories of iron oxide perfusion and BBBO for each animal have been calculated using MATLAB.

Results

Feasibility of IA trans-femoral catheter-based approach to access the vertebro-basilar circulation in a rabbit model

The rabbits' vertebral arteries were accessed via a transfemoral approach with clinically used 4-French catheters. The smaller caliber distal V4 segment and basilar artery were sufficiently large to accommodate

a 1.7-French microcatheter and maintain antegrade flow. Positioning of the 4-French catheter and microcatheter within the rabbits' vertebro-basilar system was performed safely and efficiently using fluoroscopic guidance (Supplement Figure 1a–d).

Anatomic MRI of the rabbit brain

The T2- and T1-weighted sequences provided diagnostic quality images of the brain without obscuration from the indwelling microcatheter. The horizontal and sagittal planes offered the optimal working views of the brainstem (Supplement Figure 1e, f).

DSC imaging for assessment and optimization of trans-catheter perfusion territory

DSC MRI of IA Feraheme infusions allowed real-time assessment of local parenchymal perfusion, manifested as MRI signal reduction (hypointensity) (Supplement Videos 1 and 2). Real-time DSC MRI depicted distinct areas of parenchymal perfusion, whereas conventional x-ray DSA showed perfused vasculature. Rapid Feraheme washout with clearance of the hypointensities immediately after the infusion was stopped allowed for repetitive injections at different speeds and microcatheter locations with subsequent DSC imaging; thus these parameters could be adjusted to achieve the desired perfusion territory. The dynamically acquired temporal changes in image intensity facilitated image post-processing. Subtraction perfusion images could be created and overlaid with higher resolution anatomical T2 images to provide a better appreciation of the local perfusion territory and more precise anatomical location (Figure 2b–d, i–k).

The rate of injection affected the perfusion area with slower rates producing a smaller, localized region and faster speeds resulting in a larger, more diffuse territory (Figure 3a–d). Notably, a given injection rate resulted in different ranges of perfusion territories in different rabbits, necessitating titration of injection speed to achieve the targeted area for each rabbit.

The microcatheter tip position in the vertebro-basilar circulation also affected the perfusion area with distribution to the medulla, cervical spinal cord, and adjacent paraspinal muscles when in the V4 segment (Figure 2h–k), whereas a position in the mid basilar artery resulted in supply to the pons, medulla, and cerebellum (Figure 2a–d). These territories reflect the expected anatomic arterial supply from small branches arising from the V4 segment and the basilar artery, respectively. Importantly, even small changes in the microcatheter tip position within the basilar artery resulted in differential perfusion of the brainstem based on the tortuosity and direction of flow within the basilar artery (Figure 3e–g).

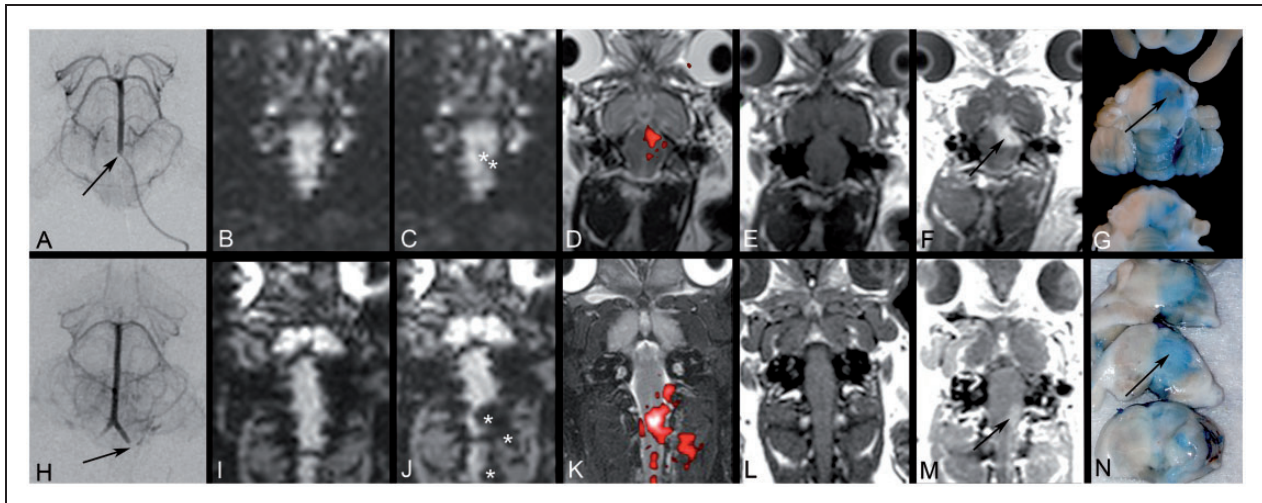


Figure 2. Focal blood–brain barrier opening (BBBO) predicted by intra-arterial injections. Microcatheter placement in the mid basilar artery (a) and V4 segment (h). The DSC MRI before (b, i) and during IA Feraheme injections (c, j) demonstrates signal intensity loss (asterisks) and the area of trans-catheter perfusion is visualized on color-coded (red) subtraction images overlaid on the T2 scan (d, k). Gadolinium enhanced T1-weighted images before (e, l) and after (f, m) intra-arterial mannitol injection demonstrate focal BBBO in the pons, cerebellum (f) and medulla (m), respectively. These areas correspond with Evans Blue extravasation (g, n).

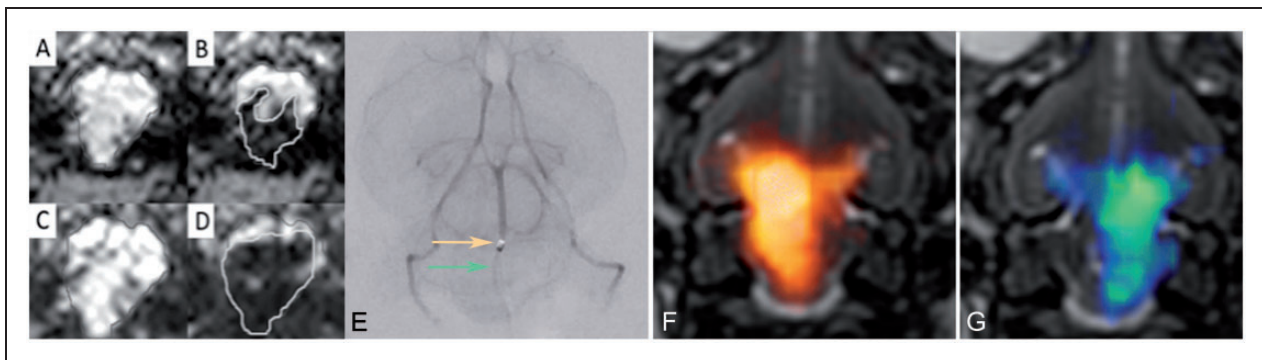


Figure 3. MRI and angiographic images demonstrating the role of infusion rate and microcatheter tip position. DSC MR images before (a, c) and during (b, d) IA Feraheme infusions at slow (a, b) and fast (c, d) rates demonstrate a larger perfusion territory with the faster infusion rate. Perfusion territory is also affected by small changes in microcatheter position even within the same vascular territory. (e) Frontal angiographic view shows a microcatheter in the mid basilar artery (orange arrow), which was subsequently withdrawn more proximally (green arrow). The two positions correspond to differential trans-catheter perfusion territories, color-coded to match the arrows (f, g).

Application of transcatheter DSC imaging and IA mannitol for precise, transient, and local BBBO

Rate of IA mannitol infusion. BBBO depended on the rate of IA mannitol infusion. IA mannitol was initially infused as short bolus injections, ranging from 0.001 to 0.26 ml/s for 30 s. This resulted in either failure to open the BBB at low rates or in respiratory depression at higher rates. Therefore, all the subsequent experiments were performed as continuous infusions from 0.001 to 0.1 ml/s for up to 15 min. If no BBBO was documented after the mannitol infusion, an additional mannitol infusion at a higher rate was administered

without delay. If BBBO was documented, no additional mannitol was infused with the exception of one rabbit described below. The 0.001 ml/s rate of infusion did not produce BBBO, even after continuous infusion for up to 15 min. Effective opening was achieved with infusion rates of 0.005 ml/s and above. Considerable size opening of the BBB within the pons (Figure 2a–g) or the medulla (Figure 2h–n) was achieved with a continuous infusion rate of 0.01 ml/s over 10 min. Optimal infusion rates between 0.005 and 0.05 ml/s that resulted in local opening of the BBB were well tolerated while irreversible respiratory depression and BBBO in the right PCA territory in addition to brainstem BBBO were present

when IA mannitol was infused at 0.26 ml/s for 30 s. In one rabbit we initially injected mannitol at lower rate (0.005 ml/s) which resulted in a localized small region of BBBO (Supplement Figure 3a). We subsequently infused mannitol at a faster rate (0.01 ml/s), which resulted in a larger area of BBBO (Supplement Figure 3b) and demonstrating the ability to adjust the region of BBBO.

Location of microcatheter for IA mannitol infusion. Microcatheter position had substantial effect on focal BBBO, which was predicted by the DSC imaging of IA Feraheme. BBBO was localized to the medulla for catheters placed in the V4 segment whereas microcatheters in the mid basilar artery created BBBO in the pons, medulla, and cerebellum (Figure 2n, g).

BBBO using IA injection of mannitol was transient and without permanent damage. One randomly selected rabbit was survived for one day after BBBO to assess for neurologic or MRI sequelae of BBBO. The microcatheter was placed in the mid basilar artery and localized BBBO, manifested as focal gadolinium enhancement, was evident in the pons. MRI after gadolinium the next day showed neither enhancement nor signal abnormalities on the T2-weighted images. EB was administered and no EB extravasation was present on post mortem brain slices (Supplement Figure 2).

The DSC images with IA Feraheme were predictive of the BBBO area, which correlated with subsequent gadolinium enhancing regions in MRI and EB extravasation (Figure 2).

Analysis for validation of procedure. We found that PPV = 69.65%, NPV = 96.73%, sensitivity = 87.13% and specificity = 90.94%. This suggests that by using transcatheter infusion of iron oxide and DSC MRI, we are able to predict at almost 70% certainty, the exact location of BBBO and we are able to predict at above 95% certainty where the BBB will remain intact. This method is further characterized by very high sensitivity = 87%, and specificity 91%.

Correlational analysis. The *r* Pearson correlation coefficient for consecutive animals equaled: 0.68, 0.81, 0.69, 0.76, 0.67, 0.70, 0.85, and each value is statistically significant ($p < 0.05$).

Discussion

Therapeutic agent delivery to the CNS is markedly impaired by an intact BBB, further diminishing the curative options for primary and metastatic tumors.⁶ Although osmotic BBBO was introduced over 40 years ago,⁷ its variability and lack of techniques for

non-invasive validation in real-time during the procedure have limited its utility and currently only a few trials have implemented this strategy.^{8,9} Alternative new methods to overcome this barrier are currently being developed and include convection-enhanced delivery,¹⁰ however drawbacks of this technique include peri-tumoral leakage¹¹ and the need for burr-hole placement. MRI guided high-intensity focused ultrasound (HIFU) is another strategy that utilizes acoustic ultrasound to induce mechanical stress and endothelial cell deformation to temporarily disrupt tight junctions, thereby increasing BBB permeability. Advantages are precise anatomic visualization and the ability to continuously monitor the tissue effect; however, the increased permeability window is narrow, which affects the scale and distribution of therapeutic molecule delivery into brain.¹²

We have achieved a satisfactory PPV near 70%. This suggests that the application of this method to IA tumor targeting, when the perfusion area is optimized to cover the entire tumor territory, would enable 70% BBBO in the tumor area. This will allow for more efficacious drug delivery via higher concentrations and greater drug penetration. This method also enhances the safety profile of the intervention as the NPV value of 95% signifies that only 5% of BBBO will occur outside the area indicated by the iron oxide infusion, limiting unintentional drug exposure of healthy parenchyma to 5%.

The larger territory highlighted on DSC MRI compared with the area of T1 enhancement is likely a result of blooming effect, which is common for susceptibility agents such as iron oxide. This artifact can potentially be reduced by further optimization of pulse sequence or/and lowering the concentration of iron oxide. This will be the subject of additional experiments aimed at further increasing the PPV, while maintaining optimal NPV.

Our work has shown that IA mannitol-induced focal BBBO can be a predictable and highly controlled procedure that can be targeted to specific regions and validated by real-time non-invasive MRI methods. These features address and reduce the major limitations of the osmotic BBBO technique. The IA route for BBBO also offers a great advantage by enabling and enhancing subsequent IA drug delivery during the same procedure.

The safety of BBBO by IA infusion of mannitol has been clinically established. Although we allowed one rabbit to survive and did not observe any toxicity manifested clinically or by MRI, that data are insufficient to make concluding statements about the toxicity and or safety of the procedure.

MRI was essential not only for BBBO validation, but also for predicting and titrating both speed of

injection and microcatheter tip position. The need to modify these parameters was evident in each animal, reflecting the flow dynamics within a specific vascular territory and each animal's individual hemodynamic variability. While microcatheter placement was performed using fluoroscopic guidance, our results emphasize the benefits of MRI and may serve as an additional impetus towards developing neurointerventional MRI technology including catheter navigation under MRI guidance. Such approach would streamline our described procedure with the added benefit of eliminating patient exposure to ionizing radiation. Indeed there is growing interest in this regard including MR-trackable catheters¹³ and/or shape sensing technology.¹⁴ As the BBB is increasingly recognized as a major limitation to effective therapies for CNS tumors, many efforts will be devoted to create innovative surgical and pharmacological strategies to circumvent it.

Conclusions

The transfemoral approach for IA mannitol-induced BBBO of the vertebro-basilar system in a rabbit model is feasible and reproducible. Non-invasive real-time BBBO validation can be accomplished with contrast-enhanced MRI. Furthermore, advanced MRI techniques, specifically DSC perfusion imaging, allow for the dynamic depiction of transcatheter parenchymal flow, which enables the prediction and titration of areas of BBBO.

Limitations of the study

1. DSC-MRI utilized for monitoring trans-catheter perfusion is related to the blooming artifact which contributes to overestimation of the targeted area. This issue can be further improved by modifying imaging parameters and concentration of the injected contrast agent.
2. Clinical utilization of MRI for neurointerventional procedures is limited due to complex MR safety issues. Prior to clinical translation, detailed testing is needed to ensure that use of IA catheters and pulse sequences are safe.
3. This pilot study is performed on a limited number of animals, however, provides strong evidence about the utility of MRI guidance for predicting localized BBBO. Further research is needed to determine the flexibility of directing transcatheter flow to fully and precisely control the area of BBBO.
4. Neurointerventional technical limitations may exist in patients. While the rabbit model was chosen because of similar aortic arch configurations and vertebro-basilar anatomy to humans, catheterization

of the vertebral and basilar arteries was relatively easy due to the absence of severe atherosclerosis, vertebral artery or basilar artery occlusion, or concomitant vascular malformations. Severe vascular occlusive disease in patients can limit transfemoral approaches and selective catheterization of one or both vertebral arteries. Additionally, severe iodine contrast allergies can limit neuroangiographic procedures.

Funding

The author(s) disclosed receipt of the following financial support for the research, authorship, and/or publication of this article: Sheik Zayed Institute for Pediatric Surgical Innovation, Children's National Medical Center, Children's Research Institute, Washington, DC and the Scholar Award in Neuroradiology Research, The Foundation of the American Society of Neuroradiology (MP). MSCRFII-0193, MSCRFII-0052, MSCRFE-0178, 2RO1 NS076573 and National Centre for Research and Development grant No 101 in ERA-NET NEURON project: "MEMS-IRBI". MJ was supported by a Kolumb Fellowship from the Foundation for Polish Science.

Declaration of conflicting interests

The author(s) declared no potential conflicts of interest with respect to the research, authorship, and/or publication of this article.

Authors' contributions

All three authors contributed to the conception and design, acquisition of data, and analysis and interpretation of data. MP drafted the initial article and all three authors participated in the revision. All authors approved the final version for publication.

Supplementary material

Supplementary material for this paper can be found at <http://jcbfm.sagepub.com/content/by/supplemental-data>.

References

1. Kroll RA and Neuwelt EA. Outwitting the blood-brain barrier for therapeutic purposes: osmotic opening and other means. *Neurosurgery* 1998; 42: 1083–1099. (discussion 99–100).
2. Budde MD, Janes L, Gold E, et al. The contribution of gliosis to diffusion tensor anisotropy and tractography following traumatic brain injury: validation in the rat using Fourier analysis of stained tissue sections. *Brain* 2011; 134: 2248–2260.
3. Peschillo S, Miscusi M and Missori P. Endovascular super-selective treatment of brain tumors: a new endovascular era? A quick review. *J Neurointervent Surg* 2015; 7: 222–224.
4. Norbash AM, Busick D and Marks MP. Techniques for reducing interventional neuroradiologic skin dose: tube position rotation and supplemental beam filtration. *AJNR Am J Neuroradiol* 1996; 17: 41–49.

5. Maeda M, Itoh S, Kimura H, et al. Tumor vascularity in the brain: evaluation with dynamic susceptibility-contrast MR imaging. *Radiology* 1993; 189: 233–238.
6. Neuwelt EA. Mechanisms of disease: the blood-brain barrier. *Neurosurgery* 2004; 54: 131–140. (discussion 41–42).
7. Rapoport SI. Effect of concentrated solutions on blood-brain barrier. *Am J Physiol* 1970; 219: 270–274.
8. Burkhardt JK, Riina H, Shin BJ, et al. Intra-arterial delivery of bevacizumab after blood-brain barrier disruption for the treatment of recurrent glioblastoma: progression-free survival and overall survival. *World Neurosurg* 2012; 77: 130–134.
9. Shin BJ, Burkhardt JK, Riina HA, et al. Superselective intra-arterial cerebral infusion of novel agents after blood-brain barrier disruption for the treatment of recurrent glioblastoma multiforme: a technical case series. *Neurosurg Clin N Am* 2012; 23: 323–329, ix–x.
10. Yin D, Zhai Y, Gruber HE, et al. Convection-enhanced delivery improves distribution and efficacy of tumor-selective retroviral replicating vectors in a rodent brain tumor model. *Cancer Gene Ther* 2013; 20: 336–341.
11. Yang X, Saito R, Nakamura T, et al. Peri-tumoral leakage during intra-tumoral convection-enhanced delivery has implications for efficacy of peri-tumoral infusion before removal of tumor. *Drug Deliv* 2015 Jul 21: 1–6. DOI: 10.3109/10717544.2014.914987.
12. Chai WY, Chu PC, Tsai MY, et al. Magnetic-resonance imaging for kinetic analysis of permeability changes during focused ultrasound-induced blood-brain barrier opening and brain drug delivery. *J Control Release* 2014; 192C: 1–9.
13. Erturk MA, El-Sharkawy AM, Moore J, et al. 7 Tesla MRI with a transmit/receive loopless antenna and B1-insensitive selective excitation. *Magn Reson Med* 2014; 72: 220–226.
14. Liu X, Iordachita II, He X, et al. Miniature fiber-optic force sensor for vitreoretinal microsurgery based on low-coherence Fabry-Perot interferometry. *Proc SPIE* 2013; 8218: 821800.